

NASF SURFACE TECHNOLOGY WHITE PAPERS
88 (10), 1-5 (October 2024)

10th Quarterly Report
April-June 2024
AESF Research Project #R-123

Electrochemical Manufacturing for Energy Applications

by
*Majid Minary Jolandan**
Department of Mechanical Engineering
The University of Texas at Dallas
Richardson, Texas, USA

Editor's Note: *The NASF-AESF Foundation Research Board selected a project on electrodeposition toward developing low-cost and scalable manufacturing processes for hydrogen fuel cells and electrolysis cells for clean transportation and distributed power applications. This report covers the tenth quarter of work, from April through June 2024.*

1. Introduction

Hydrogen has been identified by the US government as a key energy option to enable full decarbonization of the energy system.¹ The US government has recently initiated a significant investment in the Hydrogen Economy, which is detailed in the recent "Road Map to a US Hydrogen Economy: reducing emissions and driving growth across the nation" report. In June 2023, the first ever "US National Clean Hydrogen Strategy and Roadmap" was published.² On Nov. 15, 2021, President Biden signed the Bipartisan Infrastructure Law (BIL). The BIL authorizes appropriations of \$9.5B for clean hydrogen programs for the five-year period 2022-2026, including \$1B for the Clean Hydrogen Electrolysis Program. In alignment with the BIL and the mission of Hydrogen Energy "Earthshot" to reach the goal of \$1 per 1 kg in 1 decade ("1 1 1"), the US is projected to invest in priority areas that will advance domestic manufacturing and recycling of clean hydrogen technologies.

Solid oxide electrolyzer cells (SOECs) are energy storage units that produce storable hydrogen from electricity (more recently increasingly from renewable sources) and water (electrolysis of water).³ The majority (~95%) of the world's hydrogen is produced by the steam methane reforming (SMR) process that releases the greenhouse gas carbon dioxide.⁴ Electrolytic hydrogen (with no pollution) is more expensive compared to hydrogen produced using the SMR process. Investments in manufacturing and process development and increasing production scale and industrialization will reduce the cost of electrolytic hydrogen. Based on the recent DOE report, with the projected growth of the hydrogen market, the US electrolyzer capacity will have to increase by 20% compound annual growth from 2021 to 2050, with an annual manufacturing requirement of over 100 GW/yr. Given the complex structure and stringent physical and functional requirements of SOECs, additive manufacturing (AM) has been proposed as one potential technological path to enable low-cost production of durable devices to achieve economies of scale, in conjunction with the ongoing effort on traditional manufacturing fronts.⁵ Recently (2022), the PI published an article on challenges and opportunities in AM of SOCs,⁵ in which a comprehensive review of the state-of-the-art in this field is presented.

In this work, we aim to contribute to such effect of national interest to enable the hydrogen economy through development of manufacturing processes for production of low cost, durable and high efficiency solid oxide fuel cells (SOFCs) and SOECs.

* Corresponding author:

Dr. Majid Minary Jolandan
Department of Mechanical Engineering
The University of Texas at Dallas
800 West Campbell Road
Richardson, TX 75080-3021
Office: ECSW 4.355H
Phone: (972) 883-4661
Email: majid.minary@utdallas.edu

NASF SURFACE TECHNOLOGY WHITE PAPERS
88 (10), 1-5 (October 2024)

2. Summary of Accomplishments (April-June Quarter)

In this period, we followed our work on 3D printing anode support for solid oxide fuel cells, SOFC (or cathode for solid oxide electrolyzers, SOEC). We focused on the thermal shock properties of 3D printed yttria-stabilized zirconia (YSZ).

3. Activity

SOFCs and SOECs are promising players in the energy sector, generating electricity, and producing fuels with remarkable efficiency.⁶⁻⁸ However, their high-temperature operational condition, typically ranging from 600 to 800°C, presents a formidable challenge - thermal stress. These extreme temperatures, coupled with the inherent non-uniformity of heat distribution during operation, create significant thermal gradients within the cell, particularly within the electrodes.⁹ To quantitatively assess the thermal shock resistance of the porous 3D printed YSZ, the ASTM C1525-18 standard was followed.¹⁰ The thermal shock resistance of porous 3D printed YSZ was evaluated by assessing the reduction in flexural strength at different temperatures compared to the room-temperature baseline.

Figure 1A schematically illustrates the thermal shock testing procedure. Briefly, each beam underwent exposure to a high temperature for a specific duration of time, followed by rapid quenching in a DI water bath at room temperature. The beams were then dried in an oven for 4 hours at the temperature of 60°C. Subsequently, the flexural strength of the quenched beams was measured using a 4-point bending test with a Universal Testing Machine. To systematically investigate the impact of high temperature on the mechanical strength of 3D printed porous YSZ, each beam was held at the chosen temperature for 15 minutes to ensure thermal equilibrium before quenching.

The relative reduction in the flexural strength, compared to its corresponding average value at room temperature, was calculated under each thermal shock condition. According to ASTM C1525-18 standard,¹⁰ the critical temperature difference for thermal shock resistance is defined as the point in which a 30% reduction in strength occurs, compared to the room temperature average value. Accordingly, thermal shock experiments were conducted at 350°C, 500°C and 600°C to map the evolution of flexural strength as a function of exposure temperature.

Figure 1B displays the results for 3D printed porous 3YSZ before and after thermal shock. Porous YSZ beams exhibited remarkable tolerance to thermal shock up to 500°C, retaining over 70% of their flexural strength at this temperature. Beyond this point, the impact of thermal shock became more pronounced, approximately 39% reduction in strength at the maximum temperature of 600°C. Based on these observations, the critical temperature for thermal shock resistance of the porous 3D printed YSZ beams was identified as 500°C. It should be noted that despite the strength reduction, no visible surface cracks were observed on the beams at any tested temperature with naked eyes.

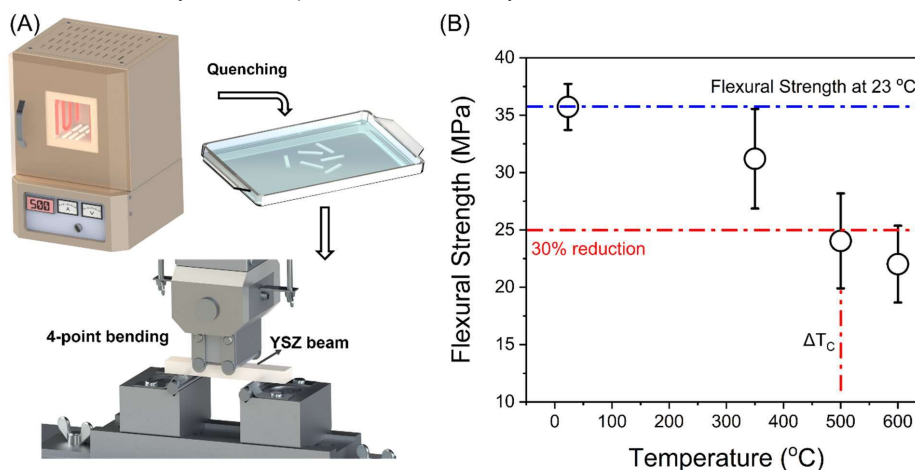


Figure 1 - (A) Schematic diagram of the thermal shock experiment followed by a 4-point bending test; (B) the measured flexural strength of the porous 3D printed YSZ beams after undergoing thermal shock at temperatures ranging from 350°C to 600°C. The top line represents the mean flexural strength of beams measured at room temperature without thermal shock, and the bottom line denotes a 30% (according to ASTM C1525-18) reduction in flexural strength compared to the room-temperature average.

NASF SURFACE TECHNOLOGY WHITE PAPERS

88 (10), 1-5 (October 2024)

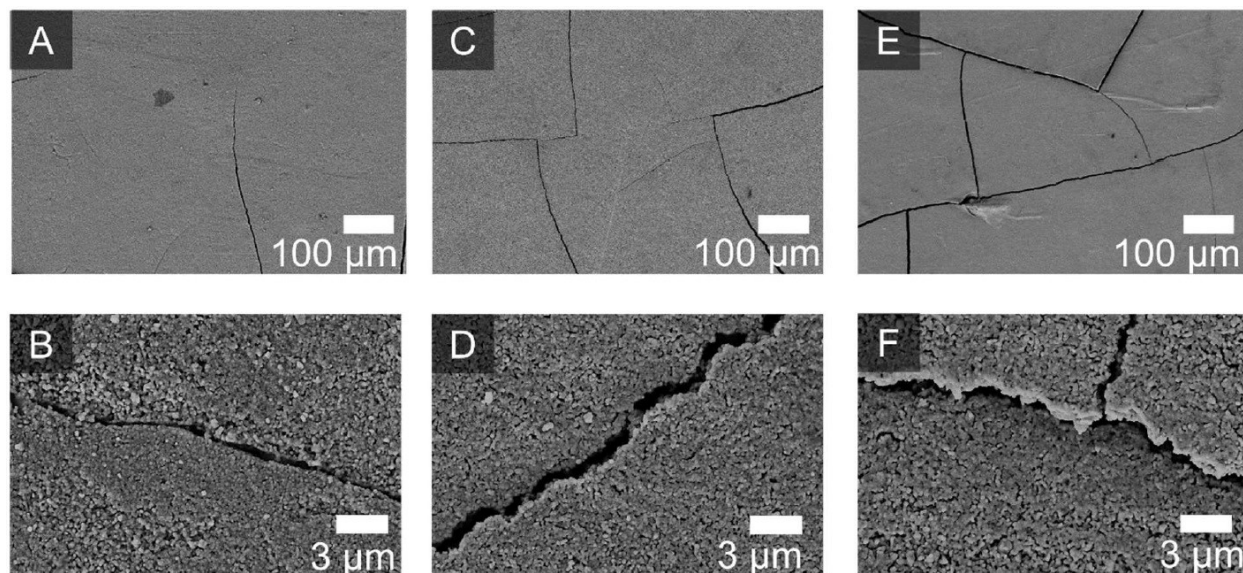


Figure 2 - SEM images of beams in the thermal shock experiment (A-B) 350°C, (C-D) 500°C and (E-F) 600°C.

To further investigate the impact of thermal shock on the microstructure of the porous 3D printed YSZ beams, SEM images were acquired (Fig. 2). The thermal shock experiment generally introduced more defects in the porous YSZ. Specifically, elevating the temperature from 350°C to 600°C during thermal shock experiments resulted in intensifying the density of cracks on the surface of the porous YSZ. The higher crack density associated with the higher thermal shock experiment caused a greater drop in the flexural strength.

Generally, the durability and strength of ceramic structures are highly dependent on their microstructural characteristics, including factors such as pore size, shape, distribution and grain size.¹¹ Research has verified that the flexural strength of spark-plasma-sintered YSZ decreased from 342.8 MPa to 43.1 MPa as porosity increased from 8% to 40.1%.¹² Similarly, Nakamura, *et al.* observed an 8.48% reduction in flexural strength for fully dense 3YSZ when grain size grew from 0.30 μm to 0.63 μm, highlighting the negative impact of larger grains on strength.¹³

While highly porous ceramics often show increased crack initiation and propagation under thermal shock, their response can be complex. It is crucial to consider both crack nucleation and the degree of damage when evaluating the influence of porosity. Literature suggested that, for porcelain-based ceramics, porosity reduced the thermal shock fracture resistance but enhanced damage resistance. This contradictory effect can be explained by the role of pores as crack arresters.^{14,15} Pores can deflect or absorb a portion of the thermal shock stress, potentially prevent crack propagation.¹⁵ Shen, *et al.* demonstrated that porous Al₂O₃/ZrO₂ ceramics with higher porosity exhibit higher critical temperature differences (ΔT_c) for thermal shock resistance compared to their less porous counterparts. For example, Al₂O₃/ZrO₂ with 6% porosity had a ΔT_c below 200°C, while increasing porosity to 31% and 43% boosted ΔT_c to 300°C and 400°C, respectively.¹⁶ Riyad, *et al.* reported for the ~45% porous 8YSZ beams a critical temperature of 400°C.¹⁷ The results of thermal shock in this study with tolerance to thermal shock of up to 500°C is significantly higher than the reported 127°C for ~98% dense 8YSZ¹⁸ and even surpasses the 325°C of 3Y-TZP (~99% dense).¹⁹

Our research currently focuses on investigating the new slurry with different packing density to create porous zirconia at final sintering temperature for application of SOCs.

4. References

1. *Achieving American Leadership in the Hydrogen Supply Chain*, US Department of Energy, 2022.
2. *US National Clean Hydrogen Strategy and Roadmap*, US Department of Energy, 2023.
3. A. Hauch, *et al.*, "Recent advances in solid oxide cell technology for electrolysis," *Science*, **370** (6513), p. eaba6118 (2020).

NASF SURFACE TECHNOLOGY WHITE PAPERS

88 (10), 1-5 (October 2024)

4. *Hydrogen Generation Market Size, Share & Trends Analysis Report By Systems Type (Merchant, Captive), By Technology (Steam Methane Reforming, Coal Gasification), By Application, By Region, And Segment Forecasts, 2022-2030*, Grand View Research, May 2022; <https://www.grandviewresearch.com/industry-analysis/hydrogen-generation-market>.
5. M. Minary-Jolandan, "Formidable Challenges in Additive Manufacturing of Solid Oxide Electrolyzers (SOECs) and Solid Oxide Fuel Cells (SOFCs) for Electrolytic Hydrogen Economy toward Global Decarbonization," *Ceramics*, **5**, 761-779 (2022); <https://doi.org/10.3390/ceramics5040055>.
6. A. Pesce, A. Hornés, M. Núñez, A. Morata, M. Torrell and A. Taracón, "3D printing the next generation of enhanced solid oxide fuel and electrolysis cells," *J. Mater. Chem. A*, **8** (33), 16926–16932 (2020); <https://doi.org/10.1039/D0TA02803G>.
7. R. Peters, R. Deja, M. Engelbracht, M. Frank, L. Blum and D. Stolten, "Efficiency analysis of a hydrogen-fueled solid oxide fuel cell system with anode off-gas recirculation," *J. Power Sources*, **328**, 105–113 (2016); <https://doi.org/10.1016/j.jpowsour.2016.08.002>.
8. Z. Masaud, *et al.*, "Recent activities of solid oxide fuel cell research in the 3D printing processes," *Trans. Korean Hydrog. New Energy Soc.*, **32** (1), 11–40 (2021); <https://doi.org/10.7316/KHNES.2021.32.1.11>.
9. Y. Wang, Y. Shi, X. Yu and N. Cai, "Thermal shock resistance and failure probability analysis on solid oxide electrolyte direct flame fuel cells," *J. Power Sources*, **255**, 377–386 (2014); <https://doi.org/10.1016/j.jpowsour.2014.01.035>.
10. ASTM, "C1525-18 Standard Test Method for Determination of Thermal Shock Resistance for Advanced Ceramics by Water Quenching," ASTM, West Conshohocken, PA, USA, 2018; <https://doi.org/10.1520/C1525-18>.
11. Y. Hirata, T. Shimonosono, T. Sameshima and S. Sameshima, "Compressive mechanical properties of porous alumina powder compacts," *Ceram. Int.*, **40** (1B), 2315–2322 (2014); <https://doi.org/10.1016/j.ceramint.2013.07.153>.
12. A. Fregeac, F. Ansart, S. Selezneff and C. Estournès, "Relationship between mechanical properties and microstructure of yttria stabilized zirconia ceramics densified by spark plasma sintering," *Ceram. Int.*, **45** (17), 23740–23749 (2019); <https://doi.org/10.1016/j.ceramint.2019.08.090>.
13. K. Nakamura, E. Adolfsson, P. Milleding, T. Kanno and U. Örtengren, "Influence of grain size and veneer firing process on the flexural strength of zirconia ceramics," *Eur. J. Oral Sci.*, **120** (3), 249–254 (2012); <https://doi.org/10.1111/j.1600-0722.2012.00958.x>.
14. D.P.H. Hasselman, "Elastic energy at fracture and surface energy as design criteria for thermal shock," *J. Am. Ceram. Soc.*, **46** (11), 535–540 (1963); <https://doi.org/10.1111/j.1151-2916.1963.tb14605.x>.
15. J. She, T. Ohji and Z. Deng, "Thermal shock behavior of porous silicon carbide ceramics," *J. Am. Ceram. Soc.*, **85** (8), 2125–2127 (2002); <https://doi.org/10.1111/j.1151-2916.2002.tb00418.x>.
16. L. Shen, M. Liu, X. Liu and B. Li, "Thermal shock resistance of the porous Al₂O₃/ZrO₂ ceramics prepared by gelcasting," *Mater. Res. Bull.*, **42** (12), 2048–2056 (2007); <https://doi.org/10.1016/j.materresbull.2007.02.001>.
17. M.F. Riyad, M. Mahmoudi and M. Minary-Jolandan, "Manufacturing and Thermal Shock Characterization of Porous Yttria Stabilized Zirconia for Hydrogen Energy Systems," *Ceramics*, **5** (3), 472–483 (2022); <https://doi.org/10.3390/ceramics5030036>.
18. J.P. Angle, J.J. Steppan, P.M. Thompson, and M.L. Mecartney, "Parameters influencing thermal shock resistance and ionic conductivity of 8 mol% yttria-stabilized zirconia (8YSZ) with dispersed second phases of alumina or mullite," *J. Eur. Ceram. Soc.*, **34** (16), 4327–4336 (2014); <https://doi.org/10.1016/j.jeurceramsoc.2014.06.020>.
19. T. Sato, M. Ishitsuka, and M. Shimada, "Thermal shock resistance of ZrO₂ based ceramics," *Mater. & Des.*, **9** (4), 204–212 (1988); [https://doi.org/10.1016/0261-3069\(88\)90032-5](https://doi.org/10.1016/0261-3069(88)90032-5).

5. Past project report

1. Quarter 1 (January-March 2022): Summary: *NASF Report in Products Finishing; NASF Surface Technology White Papers*, **86** (10), 17 (July 2022); Full paper: <http://short.pfonline.com/NASF22Jul1>.
2. Quarter 2 (April-June 2022): Summary: *NASF Report in Products Finishing; NASF Surface Technology White Papers*, **87** (1), 17 (October 2022); Full paper: <http://short.pfonline.com/NASF22Oct2>.
3. Quarter 3 (July-September 2022) **Part I**: Summary: *NASF Report in Products Finishing; NASF Surface Technology White Papers*, **87** (3), 17 (December 2022); Full paper: <http://short.pfonline.com/NASF22Dec2>.
4. Quarter 3 (July-September 2022) **Part II**: Summary: *NASF Report in Products Finishing; NASF Surface Technology White Papers*, **87** (4), 17 (January 2023); Full paper: <http://short.pfonline.com/NASF23Jan1>.
5. Quarters 4-5 (October 2022-March 2023) Summary: *NASF Report in Products Finishing; NASF Surface Technology White Papers*, **88** (1), 17 (October 2023); Full paper: <http://short.pfonline.com/NASF23Oct1>.

NASF SURFACE TECHNOLOGY WHITE PAPERS 88 (10), 1-5 (October 2024)

6. Quarter 6 (April-June 2023) Summary: *NASF Report in Products Finishing; NASF Surface Technology White Papers*, **88** (1), 17 (October 2023); Full paper: <http://short.pfonline.com/NASF23Oct2>.
7. Quarter 7 (July-September 2023) Summary: *NASF Report in Products Finishing; NASF Surface Technology White Papers*, **88** (4), 17 (January 2024); Full paper: <http://short.pfonline.com/NASF24Jan1>.
8. Quarter 8 (October-December 2023) Summary: *NASF Report in Products Finishing; NASF Surface Technology White Papers*, **88** (6), 17 (March 2024); Full paper: <http://short.pfonline.com/NASF24Mar2>.
9. Quarter 9 (January-March 2024) Summary: *NASF Report in Products Finishing; NASF Surface Technology White Papers*, **88** (9), 13 (June 2024); Full paper: <http://short.pfonline.com/NASF24June2>.

6. About the Principal Investigator for AESF Research Project #R-123



Majid Minary Jolandan is Associate Professor of Mechanical Engineering at The University of Texas at Dallas, in Richardson, Texas, in the Erik Jonsson School of Engineering. His education includes B.S. Sharif University of Technology, Iran (1999-2003), M.S. University of Virginia (2003-2005), Ph.D. University of Illinois at Urbana-Champaign (2006-2010) as well as Postdoctoral fellow, Northwestern University (2010-2012). From 2012-2021, he held various academic positions at The University of Texas at Dallas (UTD) and joined the Faculty at Arizona State University in August 2021. In September 2022, he returned to UTD as Associate Professor of Mechanical Engineering. His research interests include additive manufacturing, advanced manufacturing and materials processing.

Dr. Minary is an Associate Editor for the *Journal of the American Ceramic Society*, an Editorial Board member of *Ceramics* journal and the current chair of the materials processing technical committee of ASME.

Early in his career, he received the Young Investigator Research Program grant from the Air Force Office of Scientific Research to design high-performance materials inspired by bone that can reinforce itself under high stress. This critical research can be used for aircraft and other defense applications, but also elucidates the understanding of bone diseases like osteoporosis. In 2016, he earned the Junior Faculty Research Award as an Assistant Professor at the University of Texas-Dallas – Erik Jonsson School of Engineering.